

Proceedings of the ASME 2011 Conference on Smart Materials, Adaptive Structures and Intelligent Systems
SMASIS2011
September 18-21, 2011, Scottsdale, Arizona, USA

SMASIS2011-)%,

TESTING OF NOVEL COMPLIANT SPINES FOR PASSIVE WING MORPHING

Aimy Wissa

Ph.D. Candidate
Dept. of Aerospace Engineering
University of Maryland
National Institute of Aerospace
Hampton, VA, USA

James E. Hubbard Jr.

Langley Distinguished Professor Dept. of Aerospace Engineering University of Maryland National Institute of Aerospace Hampton, VA, USA

Yashwanth Tummala

Ph.D. Candidate
Dept. of Mechanical and Nuclear Engineering
The Pennsylvania State University
University Park, PA, USA

Mary Frecker

Professor Dept. of Mechanical and Nuclear Engineering The Pennsylvania State University University Park, PA, USA

Alexander Brown

Ph.D. Candidate
Dept. of Aerospace Engineering
University of Maryland
National Institute of Aerospace, Hampton, VA, USA

ABSTRACT

Flapping wing Unmanned Aerial Vehicles (UAVs) or ornithopters are proliferating in both the civil and military markets. Ornithopters have the potential to combine the agility and maneuverability of rotary wing aircraft with excellent performance in low Reynolds number flight regimes. These traits promise optimized performance over multiple mission scenarios. Nature achieves this broad performance in birds using wing gaits that are optimized for a particular flight regime. The goal of this work is to improve the performance of ornithopters during steady level flight by passively implementing the Continuous Vortex Gait (CVG) found in natural avian flyers. In this paper we present new experimental results for a one degree of freedom (1DOF) compliant spine which was inserted into an experimental test ornithopter leading edge wing spar in order to achieve the

desired kinematics. The lift and thrust along with electric power metrics at different flapping frequencies were measured using a six-channel load cell and a current senor, respectively. These metrics were determined for the test ornithopter both with and without the compliant spine insert. Initial results validate the ability of our compliant spine design to withstand the loads seen during flight at flapping frequencies of up to and including 5 Hz. For the ornithopter test platform used in the study, inserting the compliant spines into the wing leading edge spar accurately simulates the CVG increasing the mean lift by 16%, and reducing the power consumed by 45% without incurring any thrust penalties.

1. INTRODUCTION

Over the last few decades, flapping wing Unmanned Aerial Vehicles (UAVs), or

ornithopters, have shown the potential for advancing and revolutionizing UAV performance in both civil and military sectors [1]. An ornithopter is unique in that it can combine the agility and maneuverability of rotary wing aircraft with excellent performance in low Reynolds number flight regimes. These traits could yield optimized performance over multiple mission scenarios. Nature achieves such performance in birds using wing gaits that are optimized for a particular flight condition [2].

The goal of this work is to improve the performance of ornithopters during steady level flight using passive morphing techniques. A passive approach towards achieving wing morphing is novel. Current state of the art designs for wing morphing are either rigid-link mechanisms or they involve active morphing techniques. Many of these morphing mechanisms are rigid four-bar mechanisms [3-5]. The focus of the current paper is on the implementation of passive morphing techniques using a compliant mechanism. Not only is the proposed passive morphing novel, but when compared to active morphing mechanisms passive morphing no additional energy requires expenditure, minimal weight addition and complexity; more over there is no phase lead/lag between the flapping the morphing and mechanisms, as the morphing is only due to the aerodynamic loads experienced by the ornithopter during flight

1.1. Previous Passive Morphing Results

The benefits and efficacy of passive wing morphing by introducing an asymmetry in the leading edge wing spar geometry has been investigated. Billingsely et al. installed passive torsional springs at the wing half span to exploit the advantages of surface area reduction [6]. These springs were designed to deflect on the upstroke only and lock in place during the downstroke. Figure 1 shows nine frontal views of the wing during the wing beat cycle with the torsional springs installed. Wing bending during the upstroke reduces the wing relative area (i.e., the wing area perpendicular to the flapping motion), which in turn

mitigates the drag penalties experienced by the test ornithopter during this portion of its wing beat cycle.

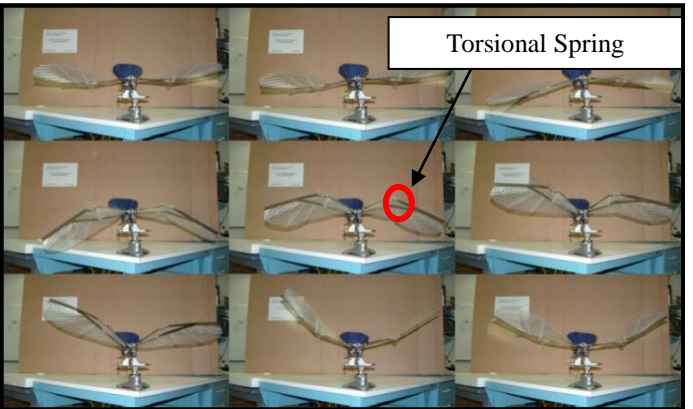


Figure 1. Test Ornithopter with Passive Torsional Spring Inserted at Wing Half Span [6].

While the results of this experiment showed a 300% increase in net lift it also induced significant thrust penalties. It was concluded that more sophisticated wing kinematics are required in order to maintain lift gains while mitigating thrust penalties to improve the overall aerodynamic performance of the ornithopter.

1.2. Proposed Passive Morphing Approach

The desired kinematics can be found in natural avian flyers and the bio-inspired gait known as the Continuous Vortex Gait (CVG) shown in Figure 2. A complete explanation of the kinematics of the CVG can be found in [3]. The advantage of using the CVG is that it is an avian gait that can be implemented passively.

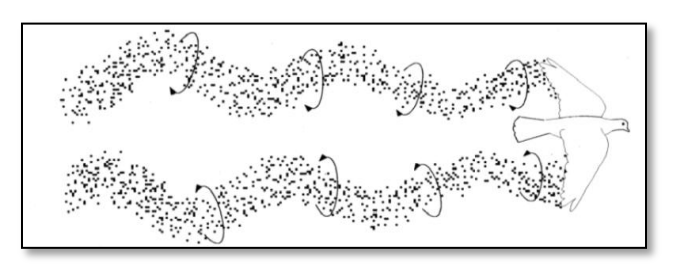


Figure 2. Continuous Vortex Gait Wake [7]

In order to implement the CVG on the test ornithopter and achieve improved performance specific wing kinematics are required. The outer

section of the wing has to bend, sweep and twist simultaneously during the upstroke, remaining fully extended during the downstroke. To attain the desired kinematics a novel compliant spine, was inserted in the leading edge wing spar at 37% of the wing half span in order to mimic the function of an avian wrist, which is the primary joint responsible for the radical shape changes in this gait. The motion described above (bending, sweep and twist) requires a 3 degree of freedom (DOF) spine. As a first step to achieving this gait a 1 DOF spine was tested in this paper. The design and optimization procedure for the 1 DOF compliant spine and its joints are explained in detail in [8] and [9]. Figure 3 shows the notional concept of the 1 DOF compliant spine with three compliant joints.



Figure 3. Conceptual Drawing of a 1 DOF Compliant Spine with 3 Compliant Joints

2. METHODOLOGY

To start the design and optimization procedure for the compliant spine, the aerodynamic loads that the spine experiences and the deflections that it needs to realize must be determined. This section discusses the methods used to measure the test ornithopter aerodynamic loads during flapping and the deflection requirements that the spine has to meet during both the up and down strokes. These requirements provided the input to the design and optimization process described in [8] and [9].

2.1. Compliant Spine Load Requirements

The strains the compliant spine would experience at a flapping frequency of 5 Hz were measured experimentally using strain gages. Two CEA-06-125UN-120 Vishay® strain gages were mounted on the leading edge spar, with their centers at the locations where the compliant spine root and

tip are located, namely 19.75 cm and 26.1 cm from the wing root. Figure 4 shows the strain gages mounted on the wing leading edge carbon fiber spar.



Figure 4. Strain Gages Mounted on the Leading Edge Spar At the Locations of the Compliant Spine Root and Tip

The strain gages were connected to a Vishay® 3800 strain indicator and the spars inserted in the test ornithopter wing. The ornithopter was flapped at 5 Hz, a typical steady level flight flapping frequency. Figure 5 shows the experimental set-up.

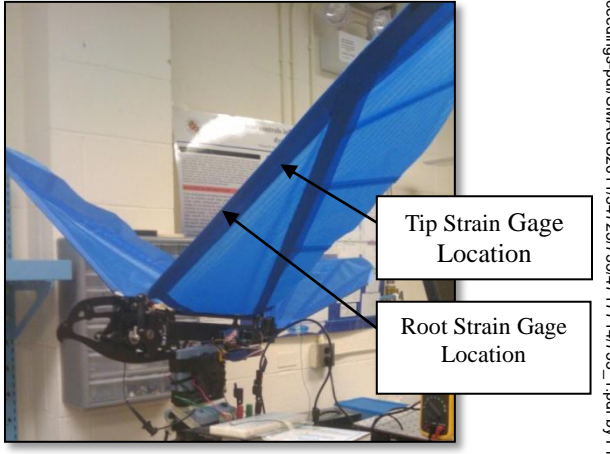


Figure 5. Experimental Set-up for Measuring The Aerodynamic Loads on the Compliant Spine

The strains at the root and tip locations were recorded for several flapping cycles. Figure 6 shows the strains measured over one flapping cycle. In the graph, the x axis is t/T which is the time, t, normalized by the flapping period, T. The normalized time parameter, t/T is zero or one at the downstroke /upstroke transition point and is 0.54 at the upstroke/downstroke transition point. The strains measured from the strain gage at the location of the root of the compliant spine will be referred to as the inboard strain, and the strain measured

from the strain gage at the location of the tip of the compliant spine is noted as the outboard strain.

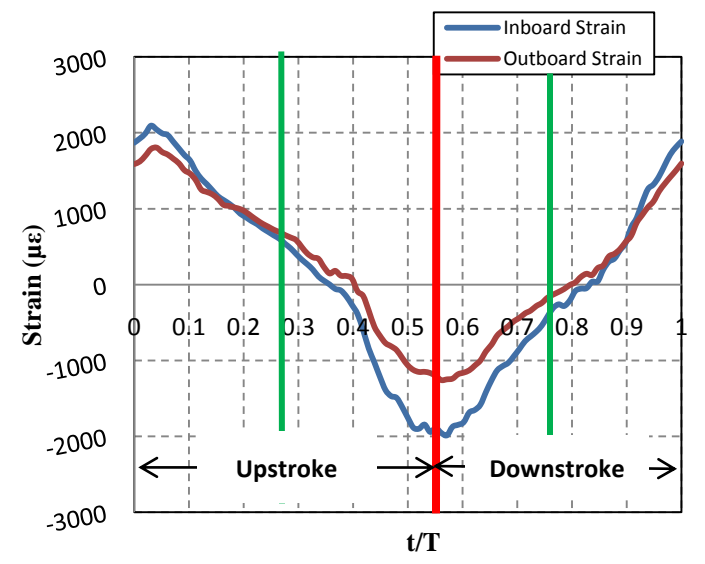


Figure 6. Inboard and Outboard Strains at the Location of the Compliant Spine Root and Tip

As shown in the above plot, there are two critical design points. The first is at the upstrokedownstroke transition point (t/T=0.54), where the maximum relative strain that the spine experiences occurs. The second critical design point is the midupstroke (t/T=0.27) when the spine is expected to deflect the most. The inboard and outboard strains shown above were used during the compliant spine design process to simulate the aerodynamic loads that this section of the spine experiences at 5 Hz [9].

2.2. Bio-inspired Deflection Requirements

After establishing the ornithopter load requirements during both the upstroke and the downstroke, the next step in the CS design process was to determine the bending deflections which a 1 DOF spine has to realize to mimic the bending kinematics of the CVG. A video of a Cockatiel flying in a wind tunnel was used to extract the required deflections [10]. Figure 7 shows nine lateral views of the Cockatiel during one wing beat cycle.

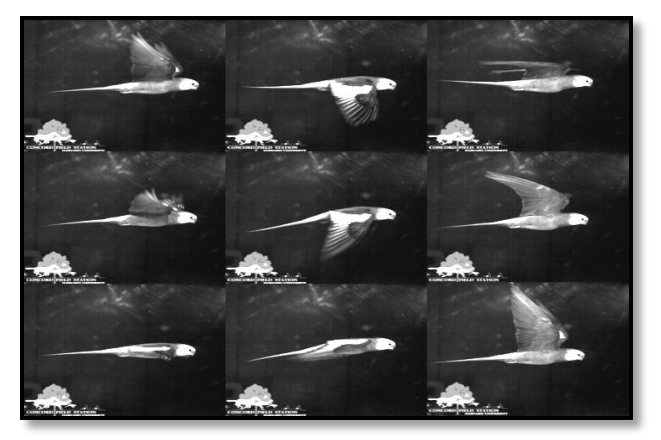


Figure 7. Lateral Flapping Sequence for a Cockatiel in a Wind Tunnel

Matlab's image processing toolbox was used to extract the wingtip sweep and bending deflections from the above images. The wingtip bending deflections were assumed to be linearly related to the deflections that the tip of the compliant spine have to realize over the flapping cycle, and were scaled accordingly. Using the wing geometry and the location of the compliant spine, the scaling factor was calculated to be 0.189. Hence the required bending deflection at the tip of the compliant spine at mid upstroke (t/T=0.25) and mid downstroke (t/T= 0.75) are 8.42 mm and 0.6 mm, respectively.

3. EXPERIMENTAL SET-UP

After specifying the load and deflection requirements for the compliant spine, a design and optimization procedure was performed. Figure 8 shows the compliant spine design that was chosen for testing. The test ornithopter performance was determined with and without the compliant spine inserted in the leading edge spars.

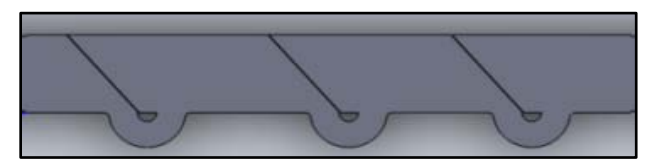


Figure 8. Tested Compliant Spine Design

There are three points of performance metrics. The first is the electric power consumed by the ornithopter. The second is the lift and thrust produced during one flapping cycle and the third is the wingtip and spine tip deflections during the up and down strokes. This section explains the experimental set-up for these three points of comparison.

3.1. Electric Power

In order to calculate the electric power, both the current and the voltage drawn from the power supply during flapping must be measured. A constant voltage power supply was used for all of the experiments, hence the supply voltage was known, V_{supply} =12.27 V.

In order to measure the current, a CQ-121E current sensor was used. The sensor was mounted in series between the power supply and the electric speed controller (ESC). Figures 9 and 10 show a picture of the current sensor and a schematic of its placement in the flapping power cycle, respectively.

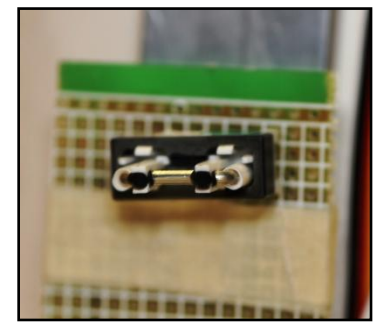


Figure 9. CQ-121E Current Sensor

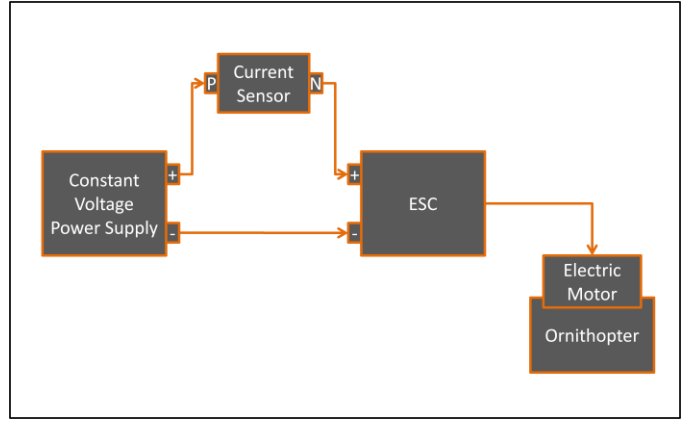


Figure 10. Schematic of Current Sensor Placement

Once the current and the voltage are measured the electric power consumed by the ornithopter at various flapping frequencies was calculated using Equation 1.

$$P = I \times V_{\text{supply}} \tag{1}$$

3.2. Lift and Thrust

The second point of comparison for this experiment is the lift and thrust metrics. A six-channel load cell was used to measure the lift and thrust produced by the test ornithopter at various flapping frequencies with and without the compliant spine inserted in the leading edge spar of its wings. Figures 11 and 12 show the test ornithopter mounted on the load cell and indicates the location of compliant spine, respectively.

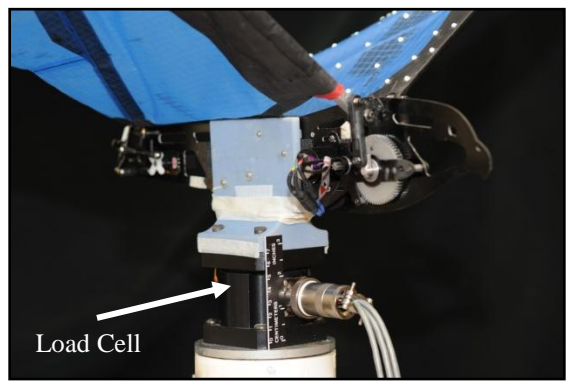


Figure 11. Ornithopter Mounted on a Six-Channel Load Cell

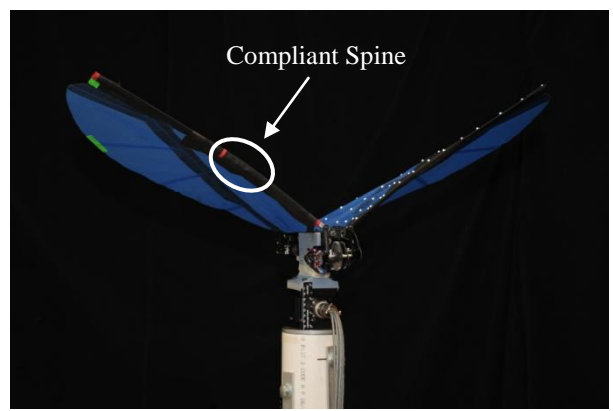


Figure 12: Ornithopter with Compliant Spines in Its Wings Mounted on a Load Cell

3.3. Wing Kinematics

The Third and last point of comparison between the test ornithopter's performance with and without the compliant spine is the wing tip and spine tip bending deflection. To capture the bending deflections of the wing during the up and downstroke, three red markers were placed on the leading edge spar. One marker was placed at the wing root, another was placed at the location of the compliant spine tip and a third marker was placed at the wing tip, as shown in Figure 13. Similarly to capture any twist deflections that occurs in the wing due to the presence of the compliant spine, two green markers were placed at the leading and trailing edges of the wing, as shown in Figure 14. Figure 15 shows the test set-up for the high speed camera used to capture the twist deflections during flapping.



Figure 13. Markers Locations for Capturing Wing Bending Deflections



Figure 14. Marker Locations for Capturing Wing Twist Deflections

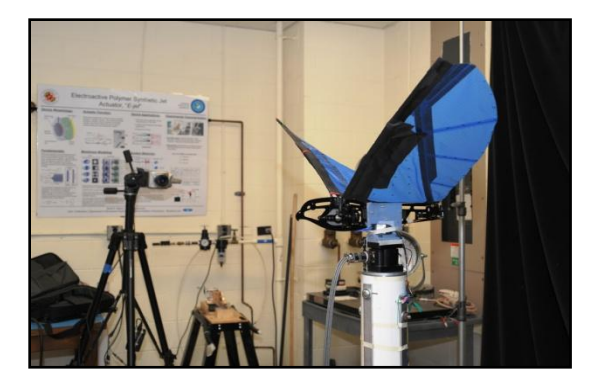


Figure 15. Lateral High Speed Camera to Capture Wing Twist

4. RESULTS

At each of the performance metrics points of comparison the effect of the compliant spine on the electric power, the lift and thrust metrics and the wing deflections is discussed.

4.1. Electric Power

As mentioned previously, the electric current was measured using a current sensor, at various flapping frequencies. The flapping frequency was controlled by the throttle position on the remote control radio transmitter. Figure 16 shows the electric power consumed by the ornithopter versus the flapping frequency for both the solid carbon fiber leading edge wing spar, and the carbon fiber spar with the compliant spine inserted.

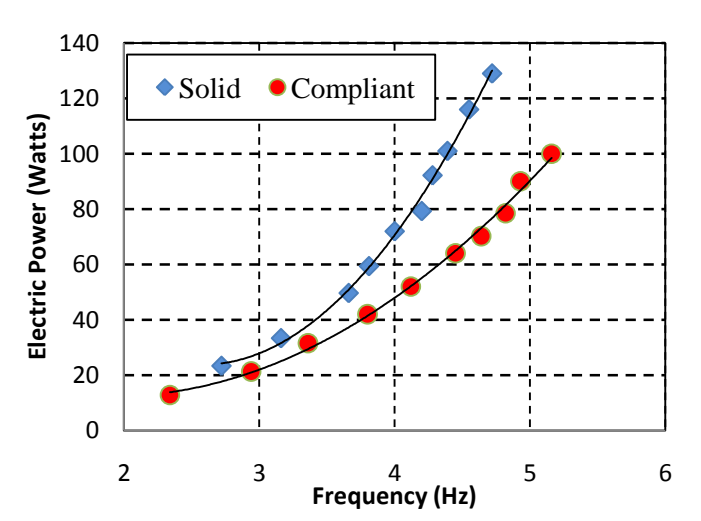


Figure 16. Electric Power versus Flapping Frequency for the Solid and Compliant Spars

From the figure above, the test ornithopter consumes less power with the compliant spine insert than it does without it for all flapping frequencies. However the focus of this work is on steady level flight and for the ornithopter tested in this experiment the flapping frequency of interest has been determined to be 4.7 Hz [11]. At 4.7 Hz the power saving due to the presence of the compliant spine is 44.7%. Also due to this power expenditure reduction, it was noticed that for a given throttle input, the ornithopter flapped at a higher frequency. Flapping at a higher frequency, as will be shown later, can produce lift and thrust improvements. Figure 17 shows the test ornithopter flapping frequency versus throttle position.

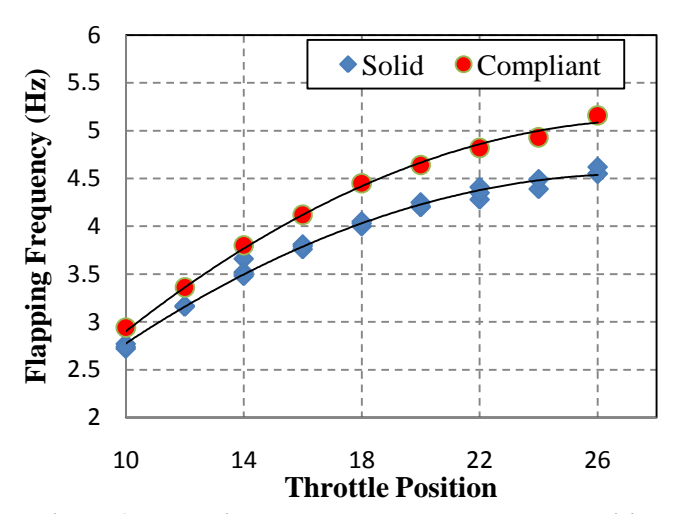


Figure 17. Flapping Frequency versus Throttle Position

4.2. Load Cell Experiment

Lift and thrust metrics as measured using a 6 DOF load cell were investigated at various flapping frequencies for one wing beat cycle. The mean lift and thrust over one flapping cycle was calculated and the mean lift was normalized by the test ornithopter's weight.

4.2.1.Mean Lift

Previous work [11] has determined that the mean induced lift produced by the test ornithopter when it is clamped to the load cell at zero forward speed and zero angle of attack is in fact zero. This is due to the symmetry between the up and down

strokes thus causing the ornithopter to produce an equal amount of positive and negative lift during the down and up strokes, respectively. The results shown in Figure 18 confirms the previous results and shows that introducing an asymmetry, by inserting the compliant spine into the wings, between the strokes causes an increase in the mean lift. Figure 18 shows that at the flapping frequency of 4.7 Hz, the ornithopter with the compliant spine produces a mean lift supporting 16% of its body weight which could not be produced under the same conditions with a solid leading edge wing spar.

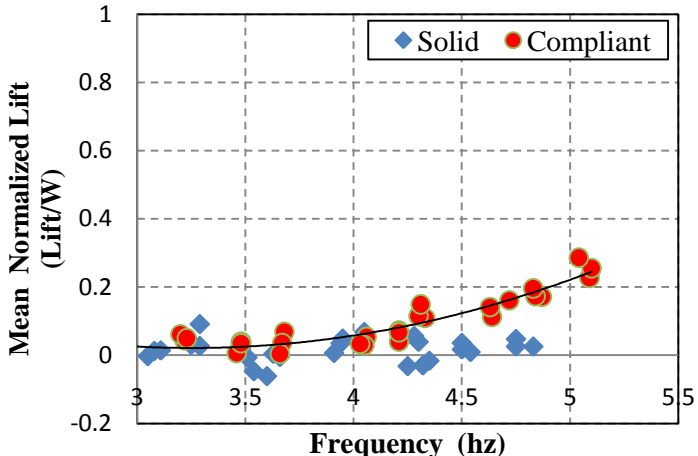


Figure 18. Mean Normalized Lift versus Flapping Frequency

Also for any given throttle position input, the ornithopter with the compliant spine insert produces more mean normalized lift, as shown in Figure 19.

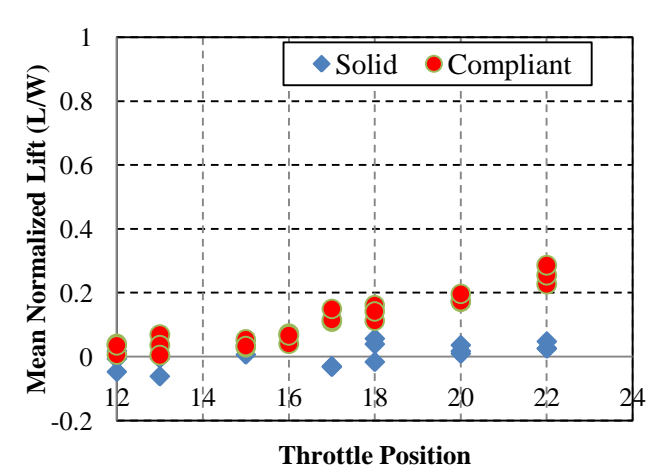


Figure 19. Mean Normalized Lift versus Throttle Position

4.2.2.Mean Thrust

Previous passive wing morphing experiments [6] showed that extreme wing bending and deflections during the upstroke can produce lift gains but also induce severe thrust penalties. The goal of this work was to maintain the lift gains while mitigating the thrust penalties. While the previous section showed 16% lift gains, this section explores the effects the compliant spine has on the mean thrust produced by the test ornithopter. Figure 20 shows that at a flapping frequency of 4.7 Hz, the mean thrust for the ornithopter with the compliant spine insert is slightly lower than the one with solid spar. The measured thrust reduction was determined to be less than 5%.

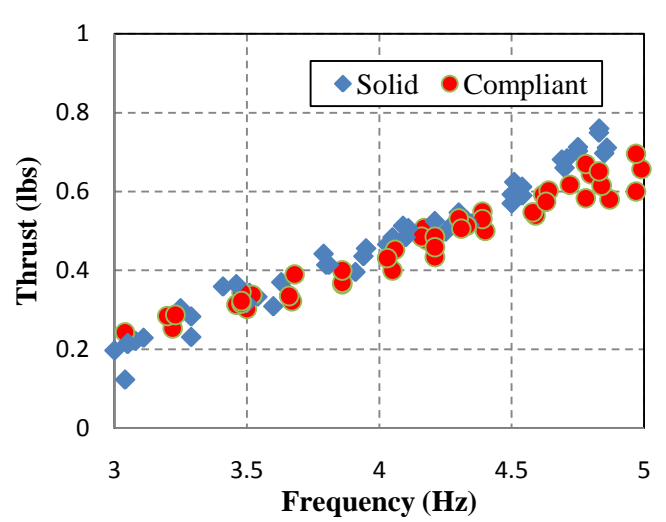


Figure 20. Mean Thrust versus Flapping Frequency

For a given throttle input, the test ornithopter with compliant spar insert flaps faster than the ornithopter with solid spar thus producing more thrust. Figure 21 shows that for any given throttle position, especially at the higher ones where the flapping frequency is of interest for steady level flight, there is no difference in the mean thrust between the solid and compliant spars. Hence we conclude that there is no real thrust penalties associated with the passive compliant design presented here.

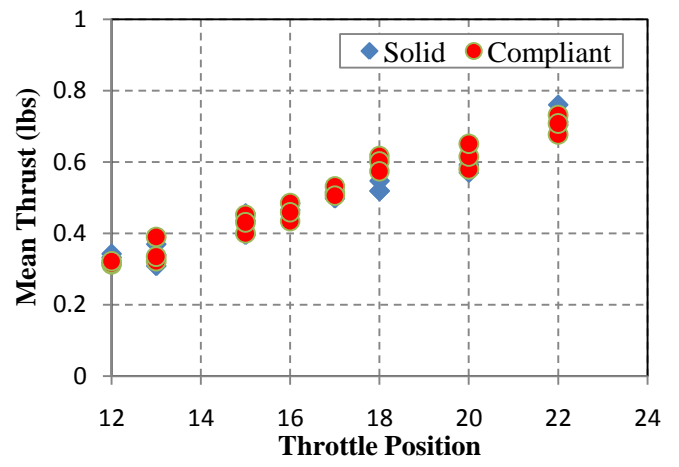


Figure 21. Mean Thrust versus Throttle Position

The compliant spine design was successful at producing lift gains without incurring any significant thrust penalties.

4.3. Wing Kinematics

Lastly the wing kinematics of the solid and compliant spars captured using high speed photography are compared. Also the compliant spine design shown in Figure 8, a 1 DOF structure, generated 2 DOF motion, namely bending and twist, during flapping. This section presents the bending and twist deflections observed due to the presence of the compliant spine.

4.3.3.Bending Kinematics

The compliant spine is designed to bend during the upstroke while remaining rigid (i.e. mimicking a solid spar) during the downstroke. Figures 22 and 23 compare the bending deflections of the compliant and solid spar at mid upstroke and mid down stroke, respectively.

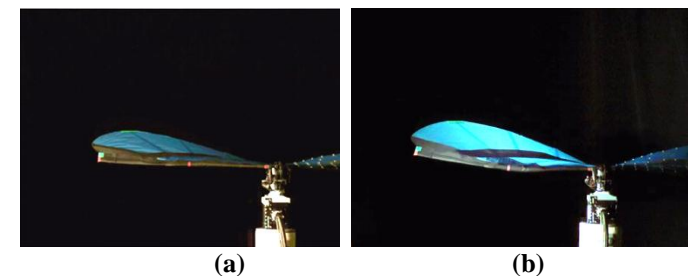


Figure 22. Mid Downstroke Bending Deflection (a) With the Solid Spar b) With the Compliant Spar



Figure 23. Mid Upstroke Bending Deflection (a) With the Solid Spar b) With the Compliant Spar

From the above figures, we conclude that the compliant spine performs as desired. During the downstroke we have minimal deflection due to the gaps between the compliant spine joints, while during the upstroke, the compliant spine bends.

4.3.4. Twist Kinematics

Even though this compliant spine is designed to induce 1 DOF motion, namely bending, twist was observed in the presence of the compliant spine. Figures 24 and 25 show the wing twist with and without the compliant spine at mid upstroke and mid down stroke, respectively.

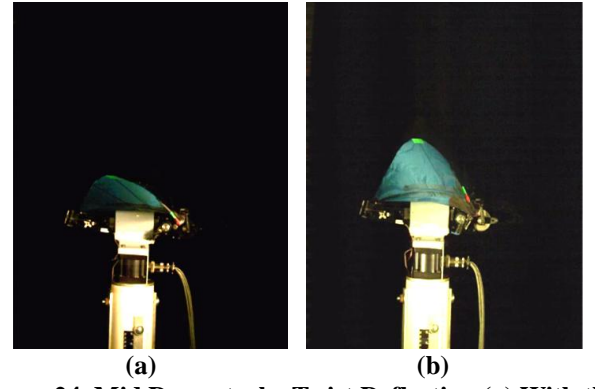


Figure 24. Mid Downstroke Twist Deflection (a) With the Solid Spar b) With the Compliant Spar

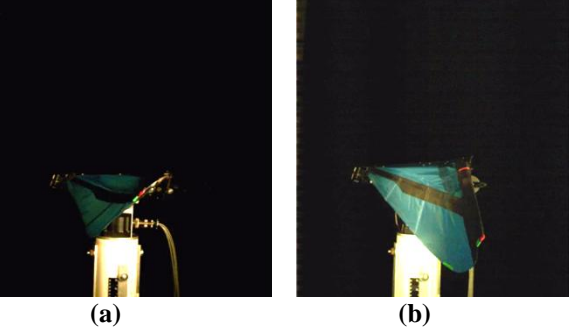


Figure 25. Mid Upstroke Twist Deflection (a) With the Solid Spar b) With the Compliant Spar

The above figures confirm that the bending deflection of the compliant spine induces twist in the ornithopter wing. During the downstroke this twist is pitch down and during the upstroke it is pitch up. Also the twist during the upstroke is more severe than the downstroke, implying that there is a relationship between the bending and twist deflections.

5. CONCLUSIONS

The compliant spine design presented here proved its capability not only to withstand the aerodynamic loads that occur on a test ornithopter at flapping frequencies of up to 5 Hz, but it also induced significant performance improvements in lift, thrust and power metrics. From an energy saving stand point, the compliant spine saved 45% of the power expenditure which can lead to significantly improved free flight range and endurance. In addition, for any given throttle input, the ornithopter with the compliant spine inserted in its wings flapped at a higher frequency than without the compliant spine. Flapping at a higher frequency for a given input leads to thrust gains as thrust is directly proportional to flapping frequency. The compliant spines presence in the wing also improved the mean lift produced by the ornithopter. The ornithopter with the compliant spine can support 16% of its weight at zero angle of attack and no forward velocity without incurring any thrust penalties. A lift gain can be viewed as a higher payload capability. Finally the 1 DOF compliant spine was able to generate a 2 DOF

motion in bending and twist, thus simplifying a final 3 DOF design objective.

6. FUTURE WORK

Future work will include quantifying the deflections captured in the videos and comparing them to those predicted by the simulation [9]. Also the effect of forward speed on the compliant spine performance from a lift, thrust and power stand point should be investigated.

7. ACKNOWLEDGMNETS

This paper is dedicated to the memory of our colleague, Alexander Brown, whom without his support and encouragement none of this work would have been possible. The authors are very grateful to have known Alex and we deeply miss him. The authors also gratefully acknowledge the support of AFOSR grant number FA9550-09-1-0632. The resources of the NASA Langley Research Center, Pennsylvania State University, the University of Maryland and the Morpheus Lab are also appreciated.

8. REFERENCES

- [1] Shyy, W., Berg, M., and Ljungqvist, D., "Flapping and flexible wings for biological and micro air vehicles," Progress in Aerospace Sciences, Vol. 35, 1999, pp. 455-505.
- [2] Tobalske, B. W. and Dial, K. P. "Flight kinematics of black-billed magpies and pigeons over a wide range of speeds," J. Exp. Biol. 1996. Vol. 199, pp. 263-280.
- [3] McDonald, M. and S.K. Agrawal, "Design of a Bio-Inspired Spherical Four-Bar Mechanism for Flapping-Wing Micro Air-Vehicle Applications," Journal of Mechanisms and Robotics, 2010. Vol. 2: p. 6.
- [4] Madangopal, R., Z.A. Khan, and S.K. Agrawal, "Biologically inspired design of small flapping wing air vehicles using four-bar mechanisms and quasi-steady aerodynamics. Journal of

- Mechanical Design," 2005. Vol. 127(4): p. 809-816.
- [5] Trease, B. and S. Kota, "Design of Adaptive and Controllable Compliant Systems with Embedded Actuators and Sensors," Journal of Mechanical Design, 2009. Vol. 131(11): p. -.
- [6] Billingsley, D., Grauer, J., Hubbard, J., "Testing of a Passively Morphing Ornithopter Wing," AIAA AUU Conference, Seattle, Washington, 6-9 April 2009.
- [7] Tobalske, B. W., "Biomechanics and physiology of gait selection in flying birds" Physiol. Biochem. Zool. 2000. Vol. 73. Pp.736–750.
- [8] Tummala, Y., Wissa A., Frecker M., Hubbard J.," Design of passively Morphing Ornithopter Wing Using a Compliant Spine," SMASIS Conference, Philadelphia, Pennsylvania, 28-30 October 2010.
- [9] Tummala, Y., Wissa A., Frecker M., Hubbard J.," Design of passively Morphing Ornithopter Wing Using a Compliant Spine," SMASIS Conference, Scottsdale Arizona, 18-21 September 2011.
- [10] Hedrick, T., Tobalske, B., Biewener, A. "Estimates of circulation and gait change based on a three dimensional kinematic analysis of flight in cockatiels (*Nymphicus hollandicus*) and ringed turtle-doves (*Streptopelia risoria*)" J. Exp. Biol. 2002. Vol. 205, pp. 1389-1409.
- [11] Harmon, R., August 2008 "Aerodynamic Modeling of Flapping Membrane Wing Using Motion Tracking Experiments", M.S. thesis, The University of Maryland